

# Exact General Relativistic Thick Disks

Guillermo A. González\*

*Escuela de Física, Universidad Industrial de Santander, A. A. 678, Bucaramanga, Colombia*

Patrício S. Letelier†

*Departamento de Matemática Aplicada, IMECC,*

*Universidade Estadual de Campinas, 13081-970 Campinas, S.P., Brazil*

A method to construct exact general relativistic thick disks that is a simple generalization of the “displace, cut and reflect” method commonly used in Newtonian, as well as, in Einstein theory of gravitation is presented. This generalization consists in the addition of a new step in the above mentioned method. The new method can be pictured as a “displace, cut, *fill* and reflect” method. In the Newtonian case, the method is illustrated in some detail with the Kuzmin-Toomre disk. We obtain a thick disk with acceptable physical properties. In the relativistic case two solutions of the Weyl equations, the Weyl gamma metric (also known as Zipoy-Voorhees metric) and the Chazy-Curzon metric are used to construct thick disks. Also the Schwarzschild metric in isotropic coordinates is employed to construct another family of thick disks. In all the considered cases we have non trivial ranges of the involved parameter that yield thick disks in which all the energy conditions are satisfied.

PACS numbers: 04.20.-q, 04.20.Jb, 04.40.-b

## I. INTRODUCTION

Exact solutions of the Einstein equations are associated to highly idealized physical systems that have some exceptional geometrical properties. In some cases with a simple exact solution one can capture a significant part of the physical properties of non trivial systems. Also, in nonlinear theories like general relativity and fluid dynamics the exact solutions play an important role in numerical analysis. These solutions can be used to test numerical codes and its outcomes. Also they can be employed as initial conditions to describe more realistic situations, e.g., a static solution can be used as part of the initial conditions for a full dynamical simulation.

Since the natural shape of an isolated self-gravitating fluid is axially symmetric, the solutions of Einstein’s field equations with this symmetry play a particularly important role in the astrophysical applications of general relativity. In particular disk like configurations of matter are of great interest, since they can be used as models of galaxies or accretion disks. Also these disks can be used as starting point to represent more realistic models in which the bulge and halo of the galaxy are considered.

Solutions for static thin disks without radial pressure were first studied by Bonnor and Sackfield [1], and Morgan and Morgan [2], and with radial pressure by Morgan and Morgan [3]. The first solution represent disks made of pressureless dust whereas the second disks with azimuthal pressure but without radial pressure. And the third a disk made of an anisotropic fluid with nonzero radial pressure. The Bonnor-Sackfield disk has a singular

rim. These disks are finite.

Several classes of exact solutions of the Einstein field equations corresponding to static [4, 5, 6, 7, 8, 9, 10, 11] and stationary [12, 13, 14] thin disks have been obtained by different authors, with or without radial pressure. Thin disks with radial tension [15], magnetic fields [16] and magnetic and electric fields [17] have been also studied. The non linear superposition of a disk and a black hole was first considered by Lemos and Letelier [7]. This solution and its generalizations has been studied in some detail in [18, 19, 20, 21, 22, 23, 24, 25]. Recently the stability of circular orbits of particles moving around black holes surrounded by axially symmetric structures have been considered in [26]. For a recent survey on relativistic gravitating thin disks, see [27].

Except for the pressureless disks all the other disks have as source matter with azimuthal pressure (tension) different from the radial pressure (tension). However, in some cases these disks can be interpreted as the superposition of two counter-rotating perfect fluids. A detailed study of the counter-rotating model for the case of static thin disks is presented in [28]. Recently, more realistic models of thin disks and thin disks with halos made of perfect fluids were considered in [29].

In all the disks mentioned above an inverse style method was used to solve the Einstein equations. The metric representing the disk is guessed and then it is used to compute the source (energy-momentum tensor). This method was named by Synge as the g-method [30] in contrast to the t-method or direct method in which the source is given and the Einstein equations are solved. The t-method, has been used to generate disks by the Jena group [31, 32, 33, 34, 35, 36, 37]. Essentially, they are obtained by solving a Riemann-Hilbert problem. These solutions are highly non trivial, but they deserve special attention because of their clear physical meaning.

---

\*e-mail: guillego@uis.edu.co

†e-mail: letelier@ime.unicamp.br

In the solutions obtained by the g-method the well known “displace, cut and reflect” method is used. The idea of the method is simple. Given a solution of the vacuum Einstein equations, a cut is made above all singularities or sources. The identification of this solution with its mirror image yields relativistic models of disks. In general, these disks are of infinite extension and finite mass.

The aim of this paper is to consider disks beyond the thin disk limit to add a new degree of reality to these geometric models of galaxies. Even though in first approximation the galactic disks can be considered to be very thin, e.g., in our Galaxy the radius of the disk is  $10\text{kpc}$  and its thickness is  $1\text{kpc}$ . In a more realistic model the thickness of the disk need to be considered. Also it is well known in fluid mechanics that the addition of a new dimension can make dramatic changes in the dynamics of the fluid. In principle, this new dimension will also change the dynamical properties of the the disk source, e.g., its stability.

In this paper we generalize the “displace, cut and reflect” method in order to obtain thick disks models from vacuum solutions of Einstein equations. We shall replace the surface of discontinuity of the metric derivatives with a “thick” shell in such a way that the matter content of the disk will be described by continuous functions with continuous first derivatives. This generalization can be named “displace, cut, *fill* and reflect” method. The disks obtained with this method, in general, will be of infinite extension and finite mass. Also as in the case of thin disks, the matter that form the thick disks will not obey simple equations of state and in some regions of the disk the pressure can change sign given rise to tensions. Although the energy condition will be fulfilled. The models of thick disks presented can be considered as generalizations of models of thin disks studied in references [17] and [29].

The article is divided as follows. In Sec. II we present, in some detail, the main idea of the “displace, cut, *fill* and reflect” method in Newtonian gravity. The method is then applied, in Sec. III, to construct relativistic thick disks in Weyl coordinates. We also study the general expression for the energy-momentum tensor of the disks. The method is illustrated by taking two simple Weyl solutions that lead to thick disks in agreement with all the energy-conditions. In Sec. IV we apply the method to the Schwarzschild solution in isotropic cylindrical coordinates. The disk obtained also satisfy all the energy conditions, this disk have equal azimuthal and radial pressures and different vertical pressure. Finally, in Sec. V, we summarize our main results.

## II. NEWTONIAN THICK DISKS

The Newtonian gravitational potential of a thin disk can be obtained by a simple procedure, the “displace, cut and reflect method”, due to Kuzmin [38]. The method

can be divided in the following steps: First, choose a surface that divides the usual space in two parts: one with no singularities or sources an the other with the sources. Second, disregard the part of the space with singularities. Third, use the surface to make an inversion of the nonsingular part of the space. The result will be a space with a singularity that is a delta function with support on  $z = 0$ . This procedure is depicted in Fig. 1.

In order to obtain a thick disk we need to modify the above procedure. We essentially need to replace the surface of discontinuity with a “thick” shell in such a way that the matter content of the disk be described by continuous functions. Now method has an additional step and can be named “displace, cut, *fill* and reflect”. After we disregard the part of the space with singularities, we put a thick shell below the surface. Then we use the bottom surface of the shell to make the inversion. The procedure is illustrated in Fig. 2.

Mathematically the method is equivalent to make the transformation  $z \rightarrow h(z) + b$ , where  $b$  is a constant and  $h(z)$  an even function of  $z$ . In Newtonian gravity, the potential  $\Phi(r, z)$  is a solution of the Laplace Equation

$$\nabla^2 \Phi = \Phi_{,rr} + \frac{\Phi_{,r}}{r} + \Phi_{,zz} = 0, \quad (1)$$

where  $(r, \varphi, z)$  are the usual cylindrical coordinates. After we make the transformation  $z \rightarrow h(z) + b$ , the above equation leads to

$$\nabla^2 \Phi = h'' \Phi_{,h} + [(h')^2 - 1] \Phi_{,hh}, \quad (2)$$

where primes indicate differentiation with respect to  $z$ .

For the case of thin disks we take  $h(z) = |z|$ . Note that  $\partial_z |z| = 2\theta(z) - 1$  and  $\partial_z \theta(z) = \delta(z)$  where  $\theta(z)$  is the Heaveside function and  $\delta(z)$  the usual Dirac distribution. By using (2), the Poisson equation leads to a mass density given by

$$2\pi G\rho(r, z) = \Phi_{,h}\delta(z). \quad (3)$$

We have a surface distribution of matter located in the plane  $z = 0$ . In Fig 3, with dashed lines, we plot  $h(z)$  an its derivatives.

For the case of thick disks the function  $h(z)$  must be selected in such a way that  $\Phi$  and its first derivatives be continuous across the plane  $z = 0$ . Let us take a function  $h(z)$  defined as

$$h(z) = \begin{cases} z - a/2 & , z \geq a, \\ z^2/2a & , -a \leq z \leq a, \\ -z - a/2 & , z \leq -a. \end{cases} \quad (4)$$

Hence, by taking the function  $h(z)$  above defined we can generate disks of thickness  $2a$  located in the region  $-a \leq z \leq a$ . In Fig. 3 we plot  $h(z)$  an its derivatives (solid lines).

When  $|z| \geq a$  the function  $h(z)$  is a linear function of  $z$  such that  $h'(z) = 1$ . Hence, its second derivative is zero.

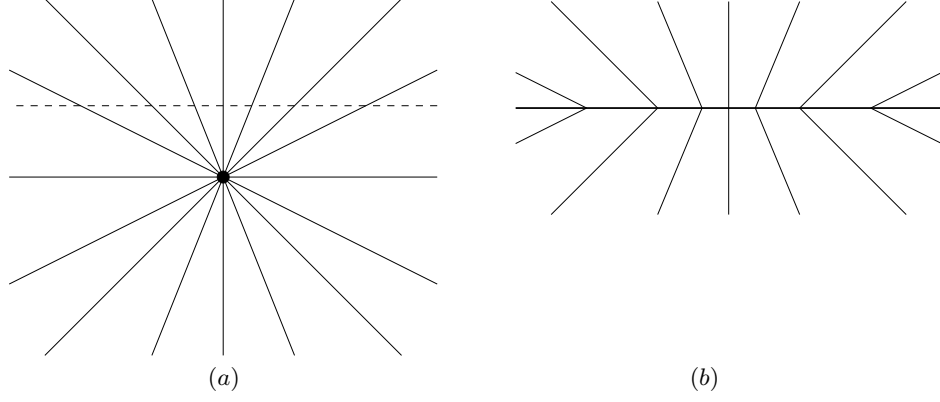


FIG. 1: Construction of a thin disk by the “displace, cut and reflect” method from the gravitational field of a mass point. In (a) the space with a singularity is displaced and cut by a plane (dashed line). In (b) the part with singularities is disregarded and the upper part is reflected on the plane.

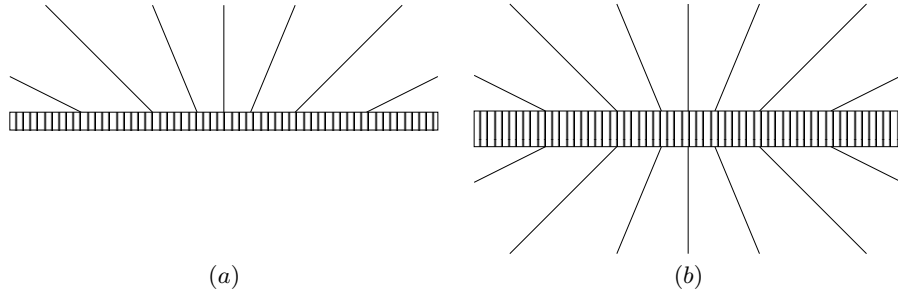


FIG. 2: Construction of a thick disk by the “displace, cut, fill and reflect” method. In (a), after disregard the part with singularities, we put a thick shell below the plane. In (b), we reflect the resultant configuration on the bottom surface of the shell.

Then the mass density vanish outside the disk. Since the first derivative is continuous at  $|z| = a$  (see Fig. 3) and the second derivative piecewise constant we have that the mass density,  $\rho$ , will be well defined inside the disk,

$$4\pi G a^2 \rho(r, z) = a\Phi_{,h} + (z^2 - a^2)\Phi_{,hh}, \quad (5)$$

for  $|z| \leq a$  and  $\rho = 0$  for  $|z| > a$ .

As a simple example we can consider the usual potential for a mass point, written in cylindrical coordinates as

$$\Phi = -\frac{Gm}{\sqrt{r^2 + z^2}}. \quad (6)$$

By doing the transformation  $z \rightarrow h(z) + b$  in the previous potential, we obtain the mass densities

$$\rho(r, z) = \frac{m b \delta(z)}{2\pi(r^2 + b^2)^{3/2}}, \quad (7)$$

for a thin disk (Kuzmin-Toomre disk [38, 39]), and

$$\begin{aligned} \rho(r, z) = & \frac{m[3z^2 + 2a(b - a)]}{8\pi a^2 R^3} \\ & + \frac{3m(a^2 - z^2)(z^2 + 2ab)^2}{16\pi a^4 R^5}, \end{aligned} \quad (8)$$

where  $R^2 = r^2 + (h + b)^2$ , for a thick disk. When  $b \geq a$ , the mass density will be positive everywhere.

The function  $h(z)$  presented in (4) is the simplest function that have the desired properties. The part of the function in the domain  $|z| \leq a$  can be changed by superposition of even functions of  $z$ . In  $|z| = a$  this new function need to be matched continuously with linear functions of  $z$  such that  $h'(z) = 1$ , like in (4). In this case the mass density can depend on the variable  $z$  in a more general way.

It is instructive to obtain the surface thin disk density (say  $\sigma$ ) associated to (7),

$$\sigma = \frac{m b}{2\pi(r^2 + b^2)^{3/2}}, \quad (9)$$

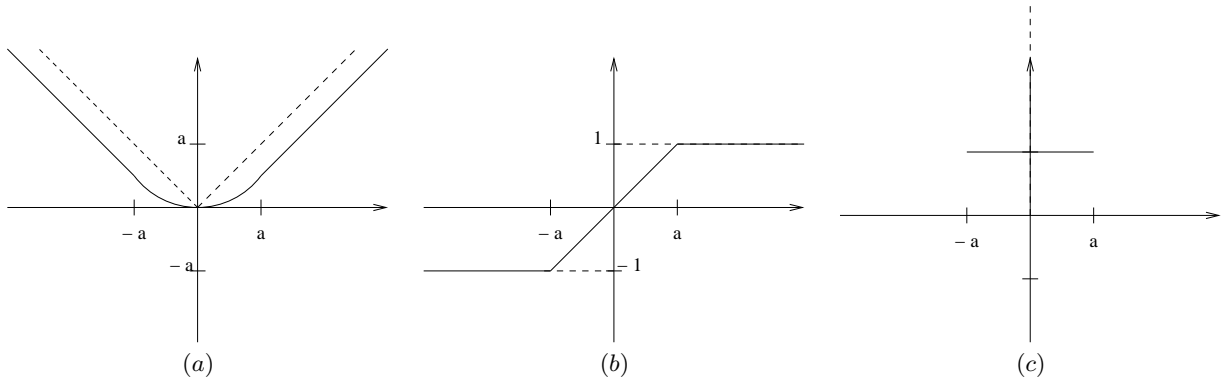


FIG. 3: The function  $h(z)$  and its derivatives, for thin disks (dashed line) and thick disks (solid line). In (a) we plot  $h(z)$ , in (b)  $h'(z)$  and in (c)  $h''(z)$ .

as a limit of the thick disk volume density (8). To obtain the surface density of the thin disk from the volume density (7) we first do

$$\Sigma = 2a\rho(r, z). \quad (10)$$

Now to perform the thin disk limit we put  $z = \alpha\xi$  and  $a = \beta\xi$  ( $\alpha$  and  $\beta$  arbitrary constants) in  $\Sigma$  and we take the limit  $\lim_{\xi \rightarrow 0} \Sigma$ . This limit is just (9).

### III. RELATIVISTIC THICK DISKS IN WEYL COORDINATES

When the matter is absent, the metric for a static axially symmetric spacetime can be cast without loosing generality as

$$ds^2 = -e^{2\Phi}dt^2 + e^{-2\Phi}[r^2d\varphi^2 + e^{2\Lambda}(dr^2 + dz^2)], \quad (11)$$

where  $\Phi$  and  $\Lambda$  are functions of  $r$  and  $z$  only. The ranges of the coordinates  $(\varphi, r, z)$  are the usual for cylindrical coordinates (Weyl coordinates) and  $-\infty \leq t < \infty$ . The Einstein vacuum equations for this metric yield the Weyl equations [40, 41],

$$\Phi_{,rr} + \frac{\Phi_{,r}}{r} + \Phi_{,zz} = 0, \quad (12a)$$

$$\Lambda_{,r} = r(\Phi_{,r}^2 - \Phi_{,z}^2), \quad (12b)$$

$$\Lambda_{,z} = 2r\Phi_{,r}\Phi_{,z}. \quad (12c)$$

From a solution of Einstein vacuum equations corresponding to a Weyl metric (11), we can construct a thick disk model by means of the “displace, cut, fill and reflect method” using the transformation  $z \rightarrow h(z) + b$ , with  $h(z)$  given by (4). The energy-momentum tensor of the

disk can be computed using the Einstein equations in the matter, written as

$$T_{ab} = R_{ab} - \frac{1}{2}g_{ab}R, \quad (13)$$

in units such that  $c = 8\pi G = 1$ .

By using the Einstein equations (12), the nonzero components of  $T_a^b$  are:

$$T_t^t = \frac{e^{2(\Phi-\Lambda)}}{a^2}[a(\Lambda_{,h} - 2\Phi_{,h}) + (z^2 - a^2)(\Phi_{,h}^2 - 2\Phi_{,hh} + \Lambda_{,hh})], \quad (14a)$$

$$T_\varphi^\varphi = \frac{e^{2(\Phi-\Lambda)}}{a^2}[a\Lambda_{,h} + (z^2 - a^2)(\Phi_{,h}^2 + \Lambda_{,hh})], \quad (14b)$$

$$T_r^r = \frac{e^{2(\Phi-\Lambda)}}{a^2}(z^2 - a^2)\Phi_{,h}^2, \quad (14c)$$

$$T_z^z = \frac{e^{2(\Phi-\Lambda)}}{a^2}(a^2 - z^2)\Phi_{,h}^2, \quad (14d)$$

valid for the region  $-a \leq z \leq a$ . Outside this region we have  $T_a^b = 0$ .

For the above expressions we can see that the radial stress  $T_r^r$  is negative (we have radial tension). On the other hand, since  $T_z^z = -T_r^r$ , we have vertical pressure. Defining the orthonormal tetrad  $\{V^b, X^b, Y^b, Z^b\}$ , where

$$V^a = e^{-\Phi} (1, 0, 0, 0), \quad (15a)$$

$$X^a = \frac{e^\Phi}{r} (0, 1, 0, 0), \quad (15b)$$

$$Y^a = e^{\Phi-\Lambda} (0, 0, 1, 0), \quad (15c)$$

$$Z^a = e^{\Phi-\Lambda} (0, 0, 0, 1), \quad (15d)$$

we can be cast the energy-momentum tensor in its canonical form

$$T_{ab} = \epsilon V_a V_b + p_\varphi X_a X_b + p_r Y_a Y_b + p_z Z_a Z_b . \quad (16)$$

Here  $\epsilon = -T_t^t$  is the energy density,  $p_\varphi = T_\varphi^\varphi$  is the azimuthal stress,  $p_r = T_r^r = -T_z^z$  is the radial tension and  $p_z = T_z^z$  is the vertical pressure.

From (14) we get the “effective Newtonian” density,  $\rho = \epsilon + p_\varphi + p_r + p_z = \epsilon + p_\varphi$ ,

$$\rho = \frac{2e^{2(\phi-\Lambda)}}{a^2} [a\Phi_{,h} + (z^2 - a^2)\Phi_{,hh}] . \quad (17)$$

The strong energy condition requires that  $\rho \geq 0$ , whereas the weak energy condition imposes the condition  $\epsilon \geq 0$ . The dominant energy condition is equivalent to the requirement  $|\frac{p_\varphi}{\epsilon}| \leq 1$ ,  $|\frac{p_r}{\epsilon}| \leq 1$  and  $|\frac{p_z}{\epsilon}| \leq 1$ , see for instance [42].

One can obtain the quantities associated to a general relativistic thin disk from the corresponding quantities associated to the thick disk using the same limit procedure described in the Newtonian disk case.

### A. Thick Disks from the Chazy-Curzon Metric

As a first example we apply the “displace, cut, fill and reflect” method to obtain thick disks using the Chazy-Curzon solution [43, 44], written in Weyl coordinates as

$$\Phi = -\frac{m}{R}, \quad (18a)$$

$$\Lambda = -\frac{m^2 r^2}{2R^4}, \quad (18b)$$

where  $R^2 = r^2 + (h+b)^2$ ,  $m$  and  $b$  are positive constants and  $h(z)$  is given by (4).

Now we rescale the variables and the parameters in terms of the disk thickness,  $a$ . We  $r = a\tilde{r}$ ,  $z = a\tilde{z}$ ,  $R = a\tilde{R}$ ,  $b = a\tilde{b}$  and  $m = a\tilde{m}$ . From (14) and (17), we obtain

$$\tilde{\rho} = \frac{\tilde{m} e^{2(\Phi-\Lambda)}}{2\tilde{R}^5} \left[ 2(3\tilde{z}^2 + 2(\tilde{b} - 1))\tilde{R}^2 + 3(1 - \tilde{z}^2)(\tilde{z}^2 + 2\tilde{b})^2 \right], \quad (19a)$$

$$\tilde{\epsilon} = \frac{\tilde{m} e^{2(\Phi-\Lambda)}}{4\tilde{R}^8} \left[ 4(3\tilde{z}^2 + 2(\tilde{b} - 1))(\tilde{R}^3 - \tilde{m}\tilde{r}^2)\tilde{R}^2 + [6(\tilde{R}^3 - 2\tilde{m}\tilde{r}^2) + \tilde{m}\tilde{R}^2](1 - \tilde{z}^2)(\tilde{z}^2 + 2\tilde{b})^2 \right], \quad (19b)$$

$$\tilde{p}_\varphi = \frac{\tilde{m}^2 e^{2(\Phi-\Lambda)}}{4\tilde{R}^8} \left[ 4\tilde{r}^2[(3\tilde{z}^2 + 2(\tilde{b} - 1))\tilde{R}^2 + 3(1 - \tilde{z}^2)(\tilde{z}^2 + 2\tilde{b})^2] + (\tilde{z}^2 - 1)(\tilde{z}^2 + 2\tilde{b})^2\tilde{R}^2 \right], \quad (19c)$$

$$\tilde{p}_r = \frac{\tilde{m}^2 e^{2(\Phi-\Lambda)}}{4\tilde{R}^6} \left[ (\tilde{z}^2 - 1)(\tilde{z}^2 + 2\tilde{b})^2 \right], \quad (19d)$$

$$\tilde{p}_z = \frac{\tilde{m}^2 e^{2(\Phi-\Lambda)}}{4\tilde{R}^6} \left[ (1 - \tilde{z}^2)(\tilde{z}^2 + 2\tilde{b})^2 \right], \quad (19e)$$

where  $\tilde{\rho} = a^2 \rho$ ,  $\tilde{\epsilon} = a^2 \epsilon$  and  $\tilde{p}_i = a^2 p_i$ .

Equation (19a) and the condition  $\tilde{b} \geq 1$  imply  $\rho > 0$ . Then, when  $\tilde{b} \geq 1$  the strong energy condition is satisfied. From (19b) we conclude that  $\epsilon \geq 0$  whenever  $\tilde{R}^3 \geq 2\tilde{m}\tilde{r}^2$  and  $\tilde{b} \geq 1$ . From the definition of  $R$  we conclude that in order to have  $\epsilon \geq 0$  everywhere, we need

$$0 \leq \tilde{m} \leq \frac{\sqrt{3}\tilde{b}}{2},$$

and  $\tilde{b} \geq 1$ .

The behavior of the densities is better illustrated graphically. In order to have a disk in agreement with the weak and strong energy conditions, we take  $\tilde{m} = 1$  and  $\tilde{b} = 2$ . In Fig. 4 we plot the effective Newtonian density and the energy density in units of  $a^2$ ,  $\tilde{\rho}$  and  $\tilde{\epsilon}$ , as

functions of  $\tilde{r}$  and  $\tilde{z}$ . We can see that the densities have a maximum at the center of the  $z = 0$  plane. Then the densities decrease monotonously as  $r$  increase and also the densities decrease for  $z \rightarrow \pm a$ . We see that  $\rho$  and  $\epsilon$  have similar magnitudes.

The azimuthal stress, as we can see from (19c), is negative at the center of the disk ( $r = 0$ ), whereas it is positive for large values of  $r$ . The boundary between the region of negative stress and positive stress is the surface

$$f(r, z) = \frac{4R^8 e^{2(\Lambda-\Phi)}}{m^2 a^2} \tilde{p}_\varphi = 0, \quad (20)$$

with  $\tilde{p}_\varphi$  given by (19c).

The behavior of the stresses is also better illustrated graphically. In Fig. 5 we plot the dimensionless azimuthal stress  $\tilde{p}_\varphi$  and vertical pressure  $\tilde{p}_z$ , as functions

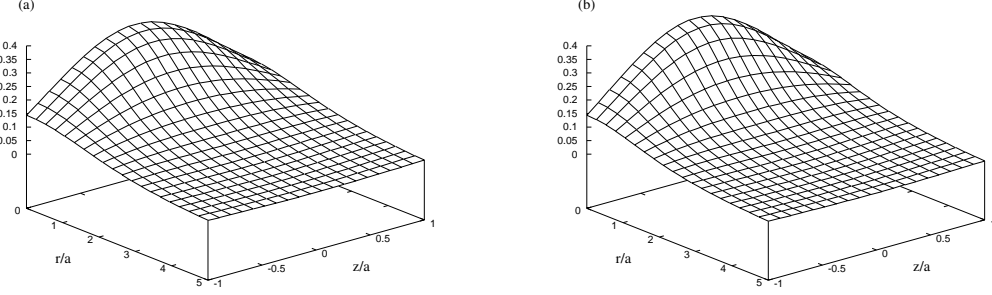


FIG. 4: For a thick disk obtained from the Chazy-Curzon solution with  $\tilde{m} = 1$  and  $\tilde{b} = 2$  we plot (a) the dimensionless Newtonian density  $\tilde{\rho}$  and (b) the dimensionless energy density  $\tilde{\epsilon}$ , as functions of  $\tilde{r}$  and  $\tilde{z}$ .

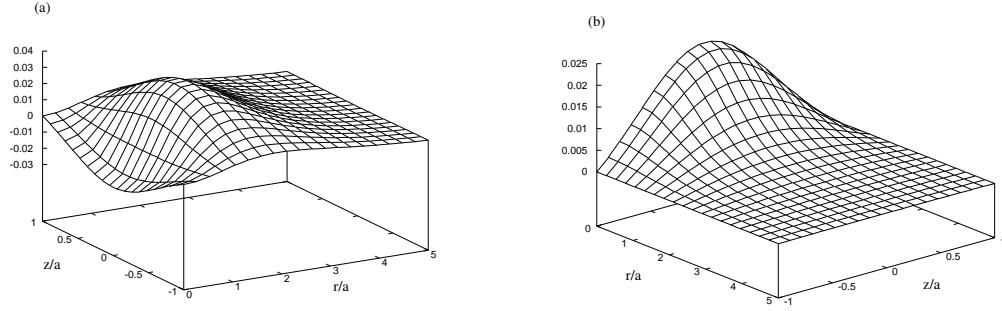


FIG. 5: For a thick disk obtained from the Chazy-Curzon solution with  $\tilde{m} = 1$  and  $\tilde{b} = 2$  we plot (a) the dimensionless azimuthal pressure  $\tilde{p}_\varphi$  and (b) the dimensionless vertical pressure  $\tilde{p}_z$ .

of  $\tilde{r}$  and  $\tilde{z}$ . The radial pressure is given by  $p_r = -p_z$ . Again we take  $\tilde{m} = 1$  and  $\tilde{b} = 2$ . The azimuthal stress is negative at the central region of the disk, then increases to have a positive maximum on the  $z = 0$  plane, for a value of  $r \approx 1.5a$ . Finally, it decreases monotonously for increasing  $r$  and also for  $z \rightarrow \pm a$ . The behavior of the vertical pressure is like of the densities, with a maximum at the center of the  $z = 0$  plane and then monotonously decreasing for increasing  $r$ . Also,  $p_z = 0$  for  $z = \pm a$ . From Figs. 4 and 5 we can also see that the magnitude of the stresses is about a tenth of the magnitude of the densities. We have

$$\left| \frac{p_\varphi}{\epsilon} \right| \leq 0.1,$$

$$\left| \frac{p_r}{\epsilon} \right| = \left| \frac{p_z}{\epsilon} \right| \leq 0.1,$$

and so the disks are also in agreement with the dominant energy condition. Thin disks based on the Chazy-Curzon metric were studied in Ref. [8].

## B. Thick Disks from the Zipoy-Voorhees Metric

As a second example we take the Weyl gamma metric also known as Zipoy-Voorhees solution [45, 46], that in Weyl coordinates can be cast as [47]

$$\Phi = \frac{m}{2k} \ln \left[ \frac{R_1 + R_2 - 2k}{R_1 + R_2 + 2k} \right], \quad (21a)$$

$$\Lambda = \frac{m^2}{2k^2} \ln \left[ \frac{(R_1 + R_2)^2 - 4k^2}{4R_1 R_2} \right], \quad (21b)$$

where  $R_1^2 = r^2 + (h + b + k)^2$ ,  $R_2^2 = r^2 + (h + b - k)^2$ ,  $m$ ,  $b$  and  $k$  are positive constants and  $h(z)$  is given by (4). When  $k = m$  this solution leads to the Schwarzschild metric and when  $k \rightarrow 0$  to the Chazy-Curzon solution of the previous section.

By using (14) and (17) we obtain, in terms of the dimensionless variables used in the previous section,

$$\tilde{\rho} = \frac{\tilde{m} e^{2(\Phi-\Lambda)}}{2\tilde{k}\tilde{R}_1^3\tilde{R}_2^3} \left\{ 2(\tilde{R}_1 - \tilde{R}_2)\tilde{R}_1^2\tilde{R}_2^2 + (1 - \tilde{z}^2) \left[ (\tilde{z}^2 + 2\tilde{b})(\tilde{R}_1^3 - \tilde{R}_2^3) - 2\tilde{k}(\tilde{R}_1^3 + \tilde{R}_2^3) \right] \right\}, \quad (22a)$$

$$\tilde{\epsilon} = \tilde{\rho} \left[ 1 - \frac{2\tilde{m}\tilde{r}^2(\tilde{R}_1 + \tilde{R}_2)}{\tilde{R}_1^2\tilde{R}_2^2[(\tilde{R}_1 + \tilde{R}_2)^2 - 4\tilde{k}^2]} \right] + \frac{\tilde{m}^2 e^{2(\Phi-\Lambda)}(1 - \tilde{z}^2)(\tilde{R}_1 - \tilde{R}_2)}{4\tilde{k}^2\tilde{R}_1^4\tilde{R}_2^4} \left[ (\tilde{R}_1 - \tilde{R}_2)\tilde{R}_1^2\tilde{R}_2^2 - 2\tilde{r}^2(\tilde{R}_1^3 - \tilde{R}_2^3) \right], \quad (22b)$$

$$\tilde{p}_\varphi = \frac{2\tilde{m}\tilde{r}\tilde{r}^2(\tilde{R}_1 + \tilde{R}_2)}{\tilde{R}_1^2\tilde{R}_2^2[(\tilde{R}_1 + \tilde{R}_2)^2 - 4\tilde{k}^2]} + \frac{\tilde{m}^2 e^{2(\Phi-\Lambda)}(\tilde{z}^2 - 1)(\tilde{R}_1 - \tilde{R}_2)}{4\tilde{k}^2\tilde{R}_1^4\tilde{R}_2^4} \left[ (\tilde{R}_1 - \tilde{R}_2)\tilde{R}_1^2\tilde{R}_2^2 - 2\tilde{r}^2(\tilde{R}_1^3 - \tilde{R}_2^3) \right], \quad (22c)$$

$$\tilde{p}_r = \frac{\tilde{m}^2 e^{2(\Phi-\Lambda)}}{\tilde{R}_1^2\tilde{R}_2^2} \left[ \frac{(\tilde{z}^2 - 1)(\tilde{z}^2 + 2\tilde{b})^2}{(\tilde{R}_1 + \tilde{R}_2)^2} \right], \quad (22d)$$

$$\tilde{p}_z = \frac{\tilde{m}^2 e^{2(\Phi-\Lambda)}}{\tilde{R}_1^2\tilde{R}_2^2} \left[ \frac{(1 - \tilde{z}^2)(\tilde{z}^2 + 2\tilde{b})^2}{(\tilde{R}_1 + \tilde{R}_2)^2} \right], \quad (22e)$$

where  $k = a\tilde{k}$ ,  $R_1 = a\tilde{R}_1$  and  $R_2 = a\tilde{R}_2$ .

From (22a) and the condition

$$A \equiv \frac{\tilde{k}(\tilde{R}_1^3 + \tilde{R}_2^3)}{(\tilde{R}_1 - \tilde{R}_2)\tilde{R}_1^2\tilde{R}_2^2} \leq 1,$$

we have  $\rho \geq 0$ , i.e., the strong energy condition is satisfied. Also from  $\tilde{R}_1^2 - \tilde{R}_2^2 = 4\tilde{k}(\tilde{h} + \tilde{b})$ , with  $\tilde{h}(\tilde{z}) = \tilde{z}^2/2$ , we can show that

$$\begin{aligned} A &= \frac{(\tilde{R}_1 + \tilde{R}_2)(\tilde{R}_1^3 + \tilde{R}_2^3)}{4(\tilde{h} + \tilde{b})\tilde{R}_1^2\tilde{R}_2^2} \\ &< \frac{\tilde{R}_1^2}{(\tilde{h} + \tilde{b})\tilde{R}_2^2} = \frac{\tilde{R}_2^2 + 4\tilde{k}(\tilde{h} + \tilde{b})}{(\tilde{h} + \tilde{b})\tilde{R}_2^2}. \end{aligned}$$

Also  $\tilde{h} + \tilde{b} \geq \tilde{b}$  and  $\tilde{R}_2 \geq \tilde{b} - \tilde{k}$  give us

$$A < \frac{(\tilde{b} - \tilde{k})^2 + 4\tilde{k}\tilde{b}}{\tilde{b}(\tilde{b} - \tilde{k})^2}.$$

Then the condition  $A \leq 1$  can be cast as

$$(\tilde{b} + \tilde{k})^2 < \tilde{b}(\tilde{b} - \tilde{k})^2, \quad (23)$$

that leads also to  $\tilde{b} \neq \tilde{k}$ . This last condition assure the nonsingular behavior of the energy density  $\epsilon$  and the azimuthal stress  $p_\varphi$ .

From (22b) and  $r = 0$  we have that  $\epsilon > 0$ . When  $\tilde{z} = 1$  the condition

$$B \equiv \frac{2\tilde{m}\tilde{r}^2(\tilde{R}_1 + \tilde{R}_2)}{\tilde{R}_1^2\tilde{R}_2^2[(\tilde{R}_1 + \tilde{R}_2)^2 - 4\tilde{k}^2]} \leq 1,$$

gives us  $\epsilon > 0$ . Since  $\tilde{R}_1 > \tilde{R}_2$ ,  $\tilde{R}_1 + \tilde{R}_2 \geq 2\tilde{b}$ ,  $\tilde{R}_2 > \tilde{r}$  and  $\tilde{R}_1 \geq \tilde{b} + \tilde{k}$  we have,

$$B < \frac{\tilde{m}}{(\tilde{b}^2 - \tilde{k}^2)(\tilde{b} + \tilde{k})}.$$

Then the condition  $B \leq 1$  leads to

$$0 < \tilde{m} < (\tilde{b}^2 - \tilde{k}^2)(\tilde{b} + \tilde{k}). \quad (24)$$

This relation yields also  $\tilde{b} > \tilde{k}$  as a condition to have  $m > 0$ .

For any other value of  $r$  and  $z$  is not easy to obtain constraints over the parameters  $\tilde{k}$ ,  $\tilde{b}$  and  $\tilde{m}$  in order to have  $\epsilon > 0$ . The analysis is better done graphically. By considering different values of  $\tilde{k}$  and  $\tilde{b}$  that fulfill the condition (23) we find that  $\epsilon > 0$  everywhere in the disks only if we take for  $\tilde{m}$  a value less than a tenth of the upper limit provided by the condition (24). As an example, in Fig. 6 we plot the dimensionless densities  $\tilde{\rho}$  and  $\tilde{\epsilon}$  for a disk with  $\tilde{m} = 3$ ,  $\tilde{b} = 3.5$  and  $\tilde{k} = 1$ . We can see that, as in the Chazy-Curzon disk, the density have a maximum at the center of the  $z = 0$  plane and then it decreases monotonously as  $r$  increase and also for  $z \rightarrow \pm a$ . Also  $\rho$  and  $\epsilon$  have similar magnitudes.

The behavior of the stresses is also similar to the presented in the Chazy-Curzon disk. Again, is better to do a graphical presentation. In Fig. 7 we plot the dimensionless azimuthal stress  $\tilde{p}_\varphi$  and the vertical pressure  $\tilde{p}_z$  for the disk with  $\tilde{m} = 3$ ,  $\tilde{b} = 3.5$  and  $\tilde{k} = 1$ . Again we have that  $p_r = -p_z$ . As with the Chazy-Curzon disk, the azimuthal stress is negative at the central region of the disk, then increase to have a positive maximum at the  $z = 0$  plane, for a value of  $r \approx 2.5a$ , and finally decrease monotonously. The behavior of the vertical pressure is like of the densities, with a maximum at the center of the  $z = 0$  plane and then monotonously decreasing for increasing  $r$ . Also,  $p_\varphi = 0$  for  $z = \pm a$ . From Fig. 6 and 7 we have

$$\left| \frac{p_\varphi}{\epsilon} \right| < 0.2,$$

$$\left| \frac{p_r}{\epsilon} \right| = \left| \frac{p_z}{\epsilon} \right| < 0.1,$$

and so the disks are also in agreement with the domi-

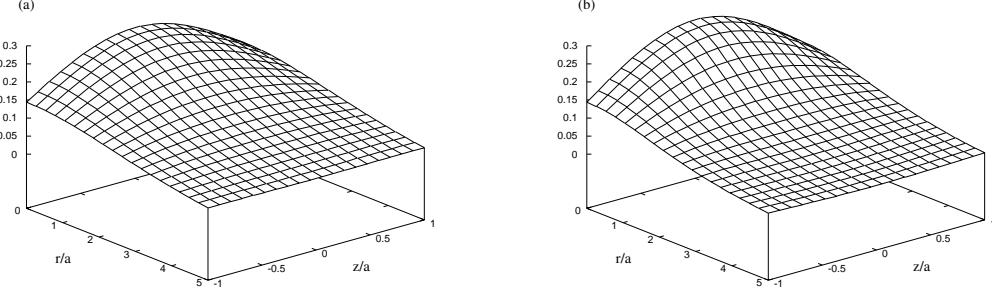


FIG. 6: For a thick disk obtained from the Zipoy-Voorhees solution with  $\tilde{m} = 3$ ,  $\tilde{b} = 3.5$  and  $\tilde{k} = 1$  we plot (a) the effective Newtonian density  $\tilde{\rho}$  and (b) the energy density  $\tilde{\epsilon}$ .

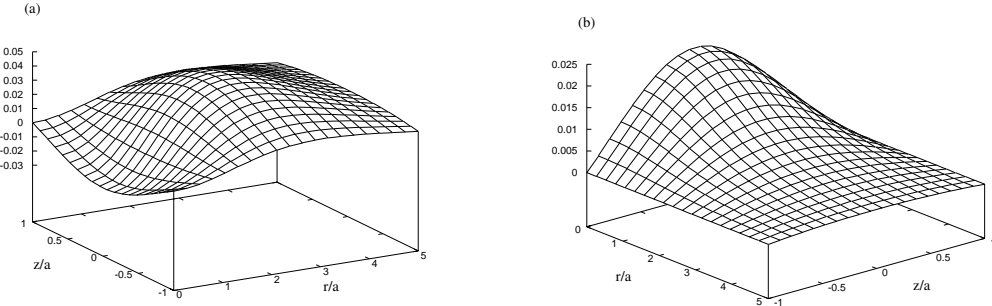


FIG. 7: For a thick disk obtained from the Zipoy-Voorhees solution with  $\tilde{m} = 3$ ,  $\tilde{b} = 3.5$  and  $\tilde{k} = 1$  we plot (a) the azimuthal stress  $\tilde{\rho}_\varphi$  and (b) the vertical pressure  $\tilde{\rho}_z$ .

nant energy condition. Thin disks based in the Zipoy-Voorhees metric were considered in Ref. [8].

#### IV. THICK DISKS FROM DE SCHWARZSCHILD METRIC IN ISOTROPIC COORDINATES

For a static spherically symmetric spacetime the metric in isotropic spherical coordinates  $(t, R, \theta, \varphi)$  can be cast as

$$ds^2 = -e^{2\Phi} dt^2 + e^{2\Lambda} [dR^2 + R^2(d\theta^2 + \sin^2 \theta d\varphi^2)], \quad (25)$$

where  $\Phi$  and  $\Lambda$  are functions of  $R$  only. In isotropic cylindrical coordinates  $(t, \varphi, r, z)$  the metric (25) takes the form

$$ds^2 = -e^{2\Phi} dt^2 + e^{2\Lambda} [r^2 d\varphi^2 + dr^2 + dz^2], \quad (26)$$

where now  $\Phi$  and  $\Lambda$  depends on  $r$  and  $z$ .

We will now apply the “displace, cut, fill and reflect” method to the Schwarzschild solution in isotropic coordinates,

coordinates,

$$\Phi = \ln \left[ \frac{2R - m}{2R + m} \right], \quad (27a)$$

$$\Lambda = \ln \left[ 1 + \frac{m}{2R} \right]^2, \quad (27b)$$

with  $m$  a positive constant and  $R^2 = r^2 + z^2$ . Now we put  $R^2 = r^2 + (h + b)^2$  where  $b$  is a positive constant and  $h(z)$  is given by (4).

From the Einstein equations (13) and the orthonormal tetrad  $\{V^a, X^a, Y^a, Z^a\}$ , where

$$V^a = e^{-\Phi} (1, 0, 0, 0), \quad (28a)$$

$$X^a = \frac{e^\Phi}{r} (0, 1, 0, 0), \quad (28b)$$

$$Y^a = e^{-\Lambda} (0, 0, 1, 0), \quad (28c)$$

$$Z^a = e^{-\Lambda} (0, 0, 0, 1), \quad (28d)$$

we find that the energy-momentum tensor of the disk can be written as

$$T_{ab} = \epsilon V_a V_b + p_\varphi X_a X_b + p_r Y_a Y_b + p_z Z_a Z_b. \quad (29)$$

Here  $\epsilon = -T_t^t$  is the energy density,  $p_\varphi = T_\varphi^\varphi$  is the azimuthal stress, that is equal to the radial stress  $p_r =$

$T_r^r$ , and  $p_z = T_z^z$  is the vertical stress. The effective Newtonian density is given by  $\rho = \epsilon + 2p_r + p_z = \epsilon + 2p_\varphi + p_z$ .

From (27) we obtain, using the dimensionless variables previously defined,

$$\tilde{\rho} = \frac{3\tilde{m}\tilde{R} \left[ 2(3\tilde{z}^2 + 2(\tilde{b} - 1))\tilde{R}^2 + 3(\tilde{z}^2 + 2\tilde{b})^2(1 - \tilde{z}^2) \right]}{(2\tilde{R} - \tilde{m})(2\tilde{R} + \tilde{m})^5}, \quad (30a)$$

$$\tilde{\epsilon} = \frac{3\tilde{m} \left[ 2(3\tilde{z}^2 + 2(\tilde{b} - 1))\tilde{R}^2 + 3(\tilde{z}^2 + 2\tilde{b})^2(1 - \tilde{z}^2) \right]}{2(2\tilde{R} + \tilde{m})^5}, \quad (30b)$$

$$\tilde{p}_\varphi = \frac{16\tilde{m}^2 \left[ (3\tilde{z}^2 + 2(\tilde{b} - 1))\tilde{R}^2 + (\tilde{z}^2 + 2\tilde{b})^2(1 - \tilde{z}^2) \right]}{(2\tilde{R} - \tilde{m})(2\tilde{R} + \tilde{m})^5}, \quad (30c)$$

$$\tilde{p}_r = \frac{16\tilde{m}^2 \left[ (3\tilde{z}^2 + 2(\tilde{b} - 1))\tilde{R}^2 + (\tilde{z}^2 + 2\tilde{b})^2(1 - \tilde{z}^2) \right]}{(2\tilde{R} - \tilde{m})(2\tilde{R} + \tilde{m})^5}, \quad (30d)$$

$$\tilde{p}_z = \frac{16\tilde{m}^2(\tilde{z}^2 + 2\tilde{b})^2(1 - \tilde{z}^2)}{(2\tilde{R} - \tilde{m})(2\tilde{R} + \tilde{m})^5}, \quad (30e)$$

From (30b) and  $\tilde{b} > 1$  we have  $\epsilon > 0$ . On the other hand, from (30a) and  $2\tilde{R} > \tilde{m}$  we have  $\rho > 0$ . Since  $\tilde{R} \geq \tilde{b}$ , this last condition is equivalent to  $2\tilde{b} > \tilde{m}$ . Therefore, when  $\tilde{b} \geq 1$  and  $0 < \tilde{m} < 2\tilde{b}$  we will have disks in agreement with the weak and strong energy conditions. Also this values of  $\tilde{m}$  assure the nonsingular behavior of  $\rho$ ,  $p_\varphi$ ,  $p_r$  and  $p_z$ . We also have  $p_\varphi = p_r > 0$  and  $p_z > 0$ . The vertical and horizontal stress are then pressures.

As in the previous section, we perform a graphical analysis of the solution. In Fig. 8 we plot  $\tilde{\rho}$  and  $\tilde{\epsilon}$  for a thick disk obtained from the Schwarzschild isotropic solution with  $\tilde{m} = \tilde{b} = 1$ . The horizontal and vertical pressures are plotted in Fig 9. All the four quantities have a similar behavior, with a maximum at the center of the  $z = 0$  plane and then monotonously decreasing with increasing  $r$  and  $z$ . The relative magnitudes of the densities and pressures are such that  $\rho \geq \epsilon \geq p_\varphi = p_r \approx p_z$ . We have

$$\left| \frac{p_\varphi}{\epsilon} \right| = \left| \frac{p_r}{\epsilon} \right| \approx \left| \frac{p_z}{\epsilon} \right| < 0.4,$$

and so the disks are in agreement with all the energy conditions. Thin disks based on the Schwarzschild solution in isotropic coordinates were studied in [29], whereas thin disks based in the Schwarzschild metric in Weyl coordinates were studied in [8]. For the disks in isotropic coordinates we have matter with radial pressure equal to the azimuthal pressure (isotropic matter) an for the disks in Weyl coordinates we have zero radial pressure.

## V. DISCUSSION

We presented a method to obtain exact general relativistic thick disks as a generalization of the “displace, cut and reflect” method commonly used to obtain Newtonian and relativistic thin disks. The generalization was be done by means of the transformation  $z \rightarrow h(z) + b$ , where  $h(z)$  is an even function of  $z$  and  $b$  is a positive constant. The function  $h(z)$  must be selected in such a way that the metric tensor and its first derivatives will be continuous across the plane  $z = 0$ .

All the cases considered leads to thick disks with similar behavior of the energy and Newtonian effective densities: a maximum at the center of the central plane of the disks, the  $z = 0$  plane, and then monotonously decreasing for increasing  $r$  and  $z$ .

We found that, when the method is applied to vacuum Weyl spacetimes, the thick disks presents radial tension and vertical pressure. The azimuthal stress is negative at the central region of the disks, then have a positive maximum and finally decrease monotonously for large values of  $r$  and  $z \rightarrow \pm a$ , where  $2a$  is the thickness of the disk. The disks obtained are in full agreement with all the energy conditions.

On the other hand, when the method is applied to the Schwarzschild isotropic metric all the stresses are pressures and have a behavior like the densities. The disks obtained are also in full agreement with all the energy

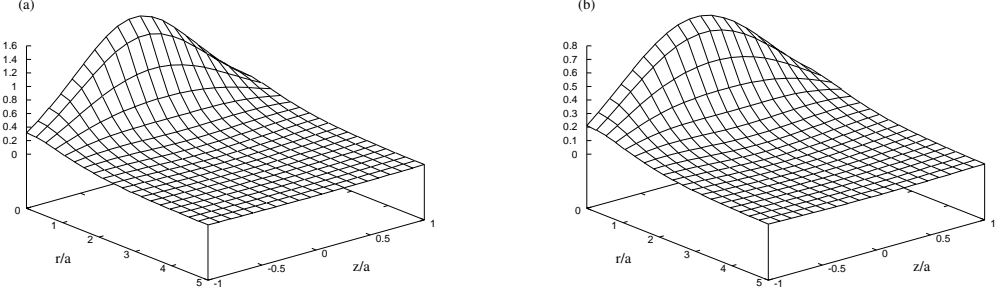


FIG. 8: For a thick disk obtained from the Schwarzschild isotropic solution with  $\tilde{m} = \tilde{b} = 1$ , we plot (a) the effective Newtonian density  $\tilde{\rho}$  and (b) the energy density  $\tilde{\epsilon}$ .

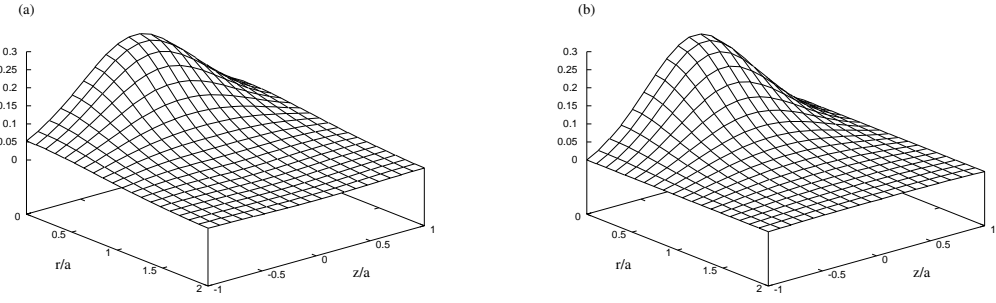


FIG. 9: For a thick disk obtained from the Schwarzschild isotropic solution with  $\tilde{m} = \tilde{b} = 1$ , we plot (a) the horizontal pressure  $\tilde{\rho}_\varphi = \tilde{\rho}_r$  and (b) the vertical pressure  $\tilde{\rho}_z$ .

conditions.

We plan to extend the models of thick disk presented along this lines by considering more elaborate functions  $h(z)$  and by the incorporation of new properties like rotation, either electric or magnetic fields or both. Also we believe that the study of stability in this disks can produce some non trivial results.

## Acknowledgments

We want to thank CNPq, FAPESP and COLCIENCIAS for financial support. Also G. A. G. is grateful for the warm hospitality of the DMA-IMECC-UNICAMP where this work was performed.

---

[1] W. A. Bonnor and A. Sackfield, Comm. Math. Phys. 8, 338 (1968).  
[2] T. Morgan and L. Morgan, Phys. Rev. 183, 1097 (1969).  
[3] L. Morgan and T. Morgan, Phys. Rev. D2, 2756 (1970).  
[4] D. Lynden-Bell and S. Pineault, Mon. Not. R. Astron. Soc. 185, 679 (1978).  
[5] P. S. Letelier and S. R. Oliveira, J. Math. Phys. 28, 165 (1987).  
[6] J. P. S. Lemos, Class. Quantum Grav. 6, 1219 (1989).  
[7] J. P. S. Lemos and P. S. Letelier, Class. Quantum Grav. 10, L75 (1993).  
[8] J. Bičák, D. Lynden-Bell and J. Katz, Phys. Rev. D47, 4334 (1993).  
[9] J. Bičák, D. Lynden-Bell and C. Pichon, Mon. Not. R. Astron. Soc. 265, 126 (1993).  
[10] J. P. S. Lemos and P. S. Letelier, Phys. Rev D49, 5135 (1994).  
[11] J. P. S. Lemos and P. S. Letelier, Int. J. Mod. Phys. D5, 53 (1996).  
[12] J. Bičák and T. Ledvinka, Phys. Rev. Lett. 71, 1669 (1993).  
[13] T. Ledvinka, M. Zofka and J. Bičák, in *Proceedings of the 8th Marcel Grossman Meeting in General Relativity*, edited by T. Piran (World Scientific, Singapore, 1999),

pp. 339-341.

[14] G. A. González and P. S. Letelier, Phys. Rev. D62, 064025 (2000).

[15] G. A. González and P. S. Letelier, Class. Quantum Grav. 16, 479 (1999).

[16] P. S. Letelier, Phys. Rev. D60, 104042 (1999).

[17] J. Katz, J. Bičák and D. Lynden-Bell, Class. Quantum Grav. 16, 4023 (1999).

[18] O. Semerák, T. Zellerin and M. Žáček, Mon. Not. R. Astron. Soc. 308, 691 (1999).

[19] O. Semerák, M. Žáček and T. Zellerin, Mon. Not. R. Astron. Soc. 308, 705 (1999).

[20] O. Semerák and M. Žáček, Class. Quantum Grav. 17, 1613 (2000).

[21] M. Žáček and O. Semerák, Publ. Astron. Soc. Japan 52, 19 (2000).

[22] O. Semerák and M. Žáček, Publ. Astron. Soc. Japan 52, 1067 (2000).

[23] O. Semerák, Class. Quantum Grav. 17, 3589 (2001).

[24] O. Semerák, Class. Quantum Grav. 19, 3829 (2002).

[25] O. Semerák, Class. Quantum Grav. 20, 1613 (2003).

[26] P. S. Letelier, *On the Stability of Circular Orbits of Particles Moving around Black Holes Surrounded by Axially Symmetric Structures*. To appear in Phys. Rev D

[27] O. Semerák, *Towards Gravitating Disks Around Stationary Black Holes*. In ‘*Gravitation: Following the Prague Inspiration*’ to celebrate the 60th birthday of Jiri Bičák, eds. O. Semerák, J. Podolsky and M. Zofka, (World Scientific, Singapore, 2002), p. 111 .

[28] G. A. González, *Relativistic Static Thin Disks: The Counter-Rotating Model*. To appear in Phys. Rev. D.

[29] D. Vogt and P. S. Letelier, *Exact General Relativistic Perfect Fluid Disks with Halos*, To appear in Phys. Rev. D.

[30] J. L. Synge, *Relativity: The General Theory*. (North Holland, 1966)

[31] C. Klein, Class. Quantum Grav. 14, 2267 (1997).

[32] G. Neugebauer and R. Meinel, Phys. Rev. Lett. 75, 3046 (1995).

[33] C. Klein and O. Richter, Phys. Rev. Lett. 83, 2884 (1999).

[34] C. Klein, Phys. Rev. D63, 064033 (2001).

[35] J. Frauendiener and C. Klein, Phys. Rev. D63, 084025 (2001).

[36] C. Klein, Phys. Rev. D65, 084029 (2002).

[37] C. Klein, Phys. Rev. D68, 027501 (2003).

[38] G. G. Kuzmin, Astron. Zh. 33, 27 (1956).

[39] A. Toomre, Astrophys. J., 138, 385 (1962).

[40] H. Weyl, Ann. Phys. 54, 117 (1917).

[41] H. Weyl, Ann. Phys. 59, 185 (1919).

[42] S. W. Hawking and G. F. R. Ellis, *The Large Scale Structure of Space-Time*. (Cambridge University Press, 1973).

[43] J. Chazy, Bull. Soc. Math. France 52, 17 (1924).

[44] H. E. J. Curzon, Proc. London Math. Soc. 23, 477 (1924).

[45] D. M. Zipoy, J. Math. Phys. 7, 1137 (1966).

[46] B. H. Voorhees, Phys. Rev. D2, 2119 (1970).

[47] H. P. Robertson and T. W. Noonan, *Relativity and Cosmology*. (Saunders, Philadelphia, 1969).